Title	Three-dimensional crystal orientation of blue phase liquid crystals on surfaces
Author(s)	Yoshida, H.; Takahashi, M.; Ohkawa, T. et al.
Citation	Proceedings of SPIE - The International Society for Optical Engineering. 2018, 10735, p. 107350I
Version Type	VoR
URL	https://hdl.handle.net/11094/76958
rights	
Note	

Three-dimensional crystal orientation of blue phase liquid crystals on surfaces

H. Yoshida*[a], M. Takahashi[a], T. Ohkawa[a], J-i. Fukuda[b], H. Kikuchi[c], and M. Ozaki[a]

[a] Dept. of Electrical, Electronic, and Information Engineering, Osaka Univ., 2-1 Yamadaoka, Suita, Osaka 565-0871 Japan

[b] Dept. of Physics, Faculty of Science, Kyushu Univ. 744 Motooka, Nishi-ku, Fukuoka 819-0395, Japan

[c] Institute for Materials Chemistry and Engineering, Kyushu Univ., 6-1 Kasuga-Koen, Kasuga, Fukuoka 816-8580, Japan

ABSTRACT

Liquid crystalline cholesteric blue phases (BPs) are of high interest for tunable electro-optic applications owing to their fast response times and quasi-polarization-independent phase modulation capabilities. Various approaches have recently been proposed to control the crystal orientation of BPs on substrates, but their basic orientation properties on standard, unidirectionally orienting substrates had not been investigated in detail. Here, detailed studies have been made on the Kossel diagrams of BPs on unidirectionally orienting substrates to understand the three-dimensional crystal orientation of BPs. We find that BPs show strong thermal hysteresis and that the structure of the preceding phase determines the orientation of BPs. Specifically, the BP II – I transition is accompanied by a rotation of the crystal such that the crystal direction defined by certain low-value Miller indices transform into different directions, and within the allowed rotations, different azimuthal configurations are obtained in the same cell depending on the thermal process. Our findings demonstrate that, for the alignment control of BPs, the thermal process is as important as the properties of the alignment layer.

Keywords: blue phase, liquid crystal, crystal orientation, phase transition, Kossel diagram

1. INTRODUCTION

Liquid crystalline cholesteric blue phases (BPs) typically appear between the cholesteric (Ch) and isotropic phases in strongly chiral liquid crystals. They are composed of so-called double-twist cylinders (DTC) in which the liquid crystal director twists in all directions perpendicular to the cylinder axis. The DTCs either stack regularly to form a crystal structure, or arrange randomly to result in a disordered structure. BPs are classified into three subphases, BP I (body-centered cubic, $I4_132$), BP II (simple cubic, $P4_232$), and BP III (disordered), depending on their symmetry [1]. While their complex structure leads to an intrinsically narrow temperature range of a few Kelvin, combining BPs with polymers or colloidal particles has proven effective in stabilizing the structure over 100 K [3-4]. The unique properties of BPs such as optical Bragg reflection [5], finite shear modulus [6], and fast electro-optic response of the Kerr type [7,8] have led to them being viewed as practical electro-optic materials with potential for various applications, from phase modulation devices, tunable photonic crystals, to biological sensors [9-11].

Despite their technological potential, the orientation behavior of BPs on substrates is not fully understood. One reason for this is that BPs are fluids with sub-micron structures, which poses difficulty in observing their structure in real space. In addition, many studies have treated BPs as an isotropic material with scalar electro-optic properties, placing little emphasis on the importance of crystal orientation. From a crystallographic point of view, however, even cubic crystals should become anisotropic upon application of external fields, and in fact, a clear anisotropy in the electro-optic coefficient has been observed in an aligned BP [12]. The influence of alignment layers on the crystal growth of BPs [13] and the optical quality of the periodic structure (enabling higher reflectances) [14] have also been reported in the literature. From both fundamental and practical viewpoints, it is important to understand the behavior of BPs on substrates.

*yoshida@eei.eng.osaka-u.ac.jp; phone +81 6 6879 7759; fax +81 6 6879 4838;

We have recently investigated the orientation of cubic BP crystals (Fig. 1) on unidirectionally orienting substrates, i.e., standard substrates used for optical applications of liquid crystals [15]. Two types of cells were prepared employing rubbing and photoalignment techniques, and the crystal orientation was investigated as BPs I and II were obtained through different thermal processes. In contrast to the many studies reporting preferential alignment of BPs I and II with the (110) and (100) crystal planes parallel to the surface [12, 20], strong thermal hysteresis was found in the orientation behavior, with different planes ((211) for BP I or (110) for BP II) becoming dominant under certain conditions. Kossel diagrams of the samples revealed a crystal rotation at the BP II − I transition such that the directions defined by certain low-value Miller indices maintain its orientation but become a direction defined by different indices. The complex behavior clearly suggests that the thermal process is as important as the properties of the alignment layer for the alignment of BPs. In this paper, we review this recent work and also report the orientation of BP I directly grown from the isotropic phase (and not through BP II) on unidirectionally orienting substrates.
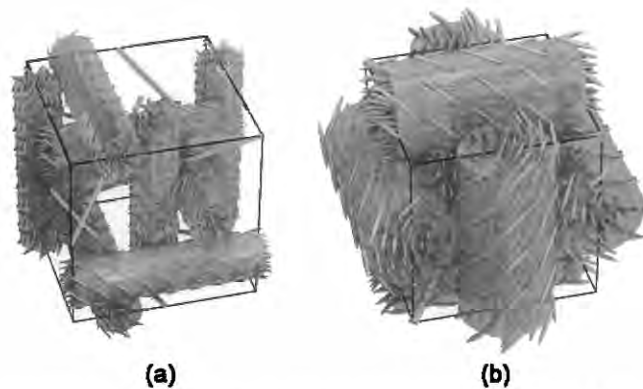

(a)   **(b)**

Figure 1. (a) Schematic illustration of BP I unit cell. The blue cylinders indication the DTCs, and the green lines indicate the disclination lines. In reality there is no "empty" region in the unit cell but is filled with liquid crystal molecules. (b) Schematic illustration of BP II unit cell.

2. EXPERIMENTAL PROCEDURE

The BP materials used in this study are shown in Table 1. Two BP materials were prepared by mixing nematic liquid crystals (5CB and JC-1041XX, both from JNC Corporation) and a right-handed chiral dopant [ISO-(6OBA)$_2$, synthesized] at different weight ratios to adjust the helical pitch. Two kinds of cells with unidirectional anchoring potentials were prepared to investigate the orientation behavior. The first cell was an anti-parallel rubbing cell (hereafter referred to as the rubbing cell), assembled from two substrates coated with polyimide (JSR, AL-1254) and rubbed by a rayon cloth (EHC Co., 20R-50). The second cell (hereafter referred to as the photoalignment cell) was prepared by coating a glass substrate with a photoalignment layer (DIC, LIA-03) and irradiating linearly polarized light (34 mW/cm^2 for 120s) after assembling the cell. Both cells had a cell-gap of approximately 9 μm.

Table 1. Composition of the BP material used in study.

Sample	Nematic liquid crystal		Chiral Dopant
	5CB	JC-1041XX	ISO-(6OBA)$_2$
BP$_{5.0\%}$	47.5	47.5	5.0
BP$_{6.5\%}$	46.75	46.75	6.5

The pretilt angles and azimuthal anchoring energies of the two cells were measured by filling the cell with the host nematic liquid crystal without the chiral dopant. The pretilt angle was measured by the crystal rotation method using a semiconductor laser as the probe light (Coherent, OBIS-640) and the azimuthal anchoring energy was determined by the torque balance method on a polarizing optical microscope (POM; Nikon, Eclipse LV100 POL). The birefringence of the host liquid crystal used for the analysis of data (described by $\Delta n = 0.141 + \dfrac{0.539 \times 10^{-2}}{\lambda^2} + \dfrac{0.846 \times 10^{-3}}{\lambda^4}$, where λ is the wavelength in micrometers) was determined by fitting the cross-polarized transmittance spectra of a planar cell with known thickness. The roughness of the alignment surfaces was measured by using an atomic force microscope (AFM; SHIMADZU, SPM-9700). The pretilt angles, azimuthal anchoring energies, and root mean square roughnesses are summarized in Table 2.

Table 2. Properties of the alignment layers [15]

	Rubbing Cell (AL1254, JSR)	Photoalignment cell (LIA-03, DIC)
Pretilt angle (°)	1.37	0.07
Azimuthal anchoring energy (J/cm^2)	13.8×10^{-6}	6.2×10^{-6}
rms roughness (nm)	12.24	3.60

The BP crystal orientation was determined from reflection micro-spectroscopy and Kossel diagram observations. The reflection spectra were measured on a POM (Nikon, Eclipse Ci-POL) using a 10× objective lens and spectrometer (Ocean Optics, USB2000) coupled to the POM by an optical fiber with diameter of 600 μm. Kossel diagrams were observed using a 100× objective lens with a numerical aperture (NA) of 0.85. The temperature of the sample was controlled using a commercial hotstage (Linkam, LTS-350).

The phase sequence of the material was first determined as the temperature was scanned at a rate of 0.1 °C/min. The dominant crystal plane orientations in each phase were then determined as the temperature was scanned again, but this time pausing in each phase to observe Kossel diagrams. To investigate the azimuthal orientation distribution of the BP crystals, a cyclic thermal treatment was applied to promote growth of the crystals [16]. Each sample was heated and cooled repetitively at a rate of 0.1 °C within the temperature range of BP $I_{(110)}$ for three hours. To describe the orientation of BPs, hereafter we write BP crystals with $(h\ k\ l)$ crystal plane orientation parallel to the substrates as $BP_{(hkl)}$, and refer to a direction $<h\ k\ l>$ in the cubic unit cell of the BP as $BP_{<hkl>}$.

3. RESULTS AND DISCUSSIONS

Figure 2 shows the phase sequence of the $BP_{6.5\%}$ material in the rubbing and photoalignment cells, along with the dominant crystal plane orientations in each phase. The BP material shows different orientations depending on the alignment layer and thermal history. On heating the sample from the cholesteric phase, BP $I_{(100)}$ and BP $II_{(100)}$ alignment is obtained in both cells. However, on cooling the sample from the isotropic phase, the rubbing cell shows BP $II_{(110)}$ and BP $I_{(211)}$ orientations, whereas the photoalignment cell shows BP $II_{(100)}$ and BP $I_{(110)}$ orientations. When the sample is first heated to BP $II_{(100)}$ and then cooled to BP I, BP $I_{(110)}$ is obtained for both cells (Fig. 2(a,c)).

The results demonstrate the sensitivity of the crystal plane orientation of BP II to the surface conditions when grown from the isotropic phase. The subtle difference in the properties of the rubbing and photoalignment cells (Table 2) leads
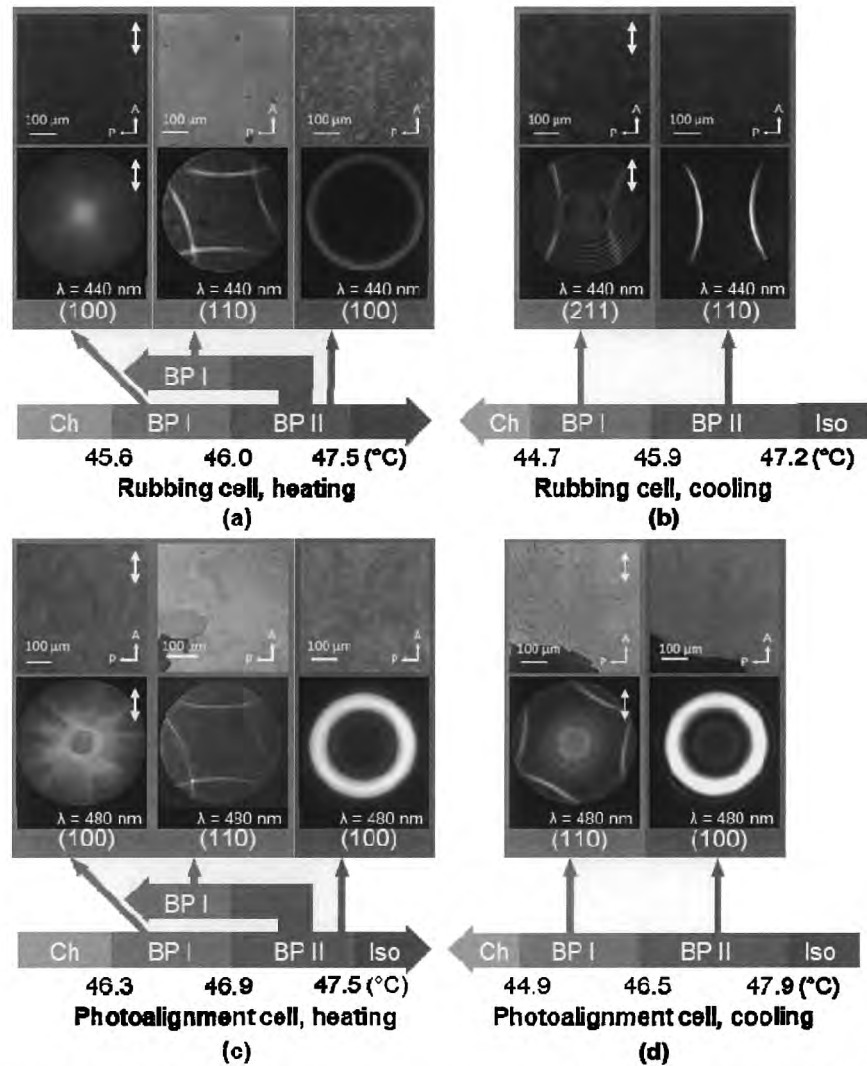
Figure 2. Phase sequence, POM image and Kossel diagrams of BPs prepared by different processes. (a) Heating and (b) cooling processes of the rubbing cell, and (c) heating and (d) cooling process of the photoalignment cell. The double-headed arrows indicate the orientational easy axis. [15]

Figure 3 shows typical Kossel diagrams of BP $I_{(110)}$ obtained by the following thermal histories: Ch → BP $I_{(100)}$ → BP $II_{(100)}$ →BP $I_{(110)}$; Ch → BP $I_{(100)}$ → BP $II_{(100)}$ → BP $I_{(110)}$; and Iso → BP $II_{(100)}$ → BP $I_{(110)}$. The two-fold axis, which corresponds to the [$\bar{1}$10] direction of the BP crystal, is tilted with respect to the orientational easy axis, and orients in different directions depending on the thermal history. Figure 3 (b) shows histograms of the azimuthal orientation angles for the three samples (measured at 20 domains in each sample), where the azimuthal angle is defined as the angle of the [$\bar{1}$10] axis from the orientational easy axis. Depending on the preparation procedure, the azimuthal orientation is narrowly distributed around either ~ 55° or 35°.

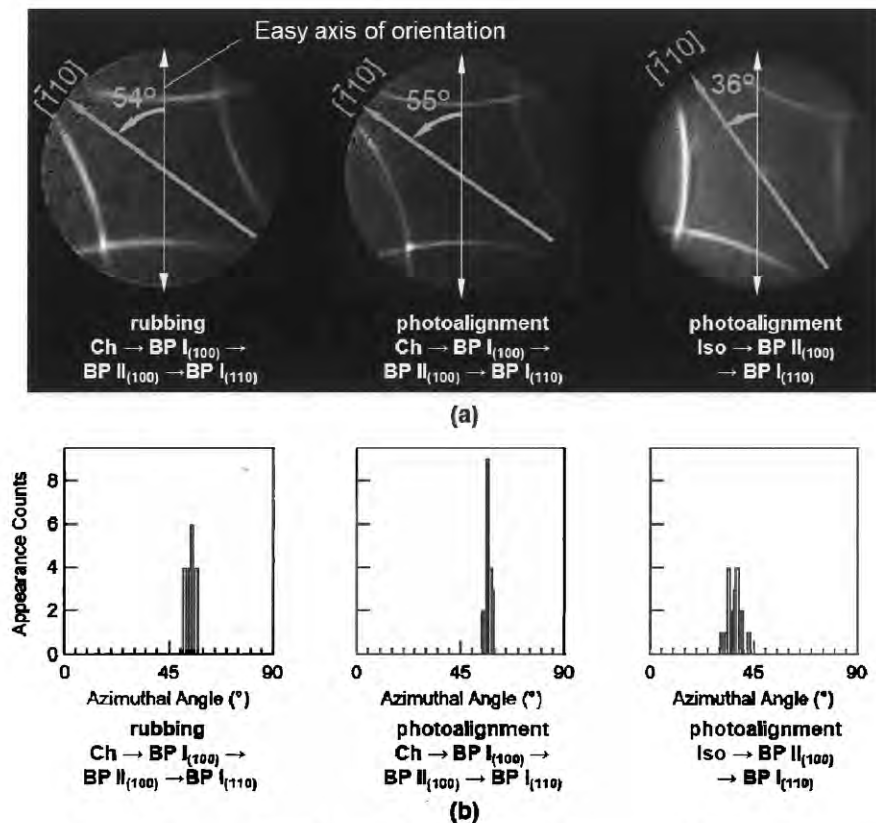Figure 3. (a) Kossel diagrams of $BP_{(110)}$ prepared through different thermal processes on different substrates. (b) Distribution of the azimuthal angle (angle of $[\bar{1}10]$ axis from the easy axis) measured at 20 points in each cell. [15]

Considering the crystal structure of BP I, we find that orientation angles of 55° and 35° correspond to cases where the $[2\bar{1}1]$ and the $[1\bar{1}1]$ axes are aligned along the orientational easy axis, and the $[\bar{1}11]$ and $[\bar{1}12]$ axes are aligned perpendicular to the easy axis, respectively. In contrast to BP $I_{(110)}$, the azimuthal orientation of BP $II_{(100)}$ cannot be determined because the Kossel diagram is featureless; however, transmission electron microscopy of polymerized BP $II_{(100)}$ has shown that the crystal is oriented with its [001] axis approximately along the easy axis on the substrate [19]. Thus, we find that the BP $II_{(100)}$ → BP $I_{(110)}$ transition occurs so that the <100> axes of BP II coincide with the <110>, <111>, and <112> axes of BP I (Fig. 4). It is not clear how the transformation of each axis is defined; for example, why the <110> axis becomes perpendicular to the substrates, and why in some cases the <112> axis is aligned along the easy axis while in other cases the <111> axis is aligned. However, we suspect that factors such as cell-gap and surface boundary conditions are affecting the behavior. We note that since the rotation of the crystal is accompanied by a change in the number of crystals present along that direction, transition into some directions are more favorable than other directions. Along the thickness direction, which typically has dimensions much smaller than the other two directions, the change in crystal number should be most disfavored. By setting this direction as <110>, the change in crystal number is minimized, since the effective lattice lengths are closest between BP $II_{<100>}$ and BP $I_{<110>}$.

We also note that because the unidirectional boundary condition is topologically incompatible with the BP structure, the BP must be deformed near the substrates. It is quite likely that this "transitional layer" is affecting the alignment behavior of BPs. The photoalignment cell shows a peculiar behavior in which two different BP $I_{(110)}$ orientations are obtained from BP $II_{(100)}$ (with either $[2\bar{1}1]$ or $[1\bar{1}1]$ axes being aligned along the easy axis) only depending on the thermal history. Such behavior cannot be explained from crystallographic arguments alone and may be a consequence of the difference in structure of the transitional layer.
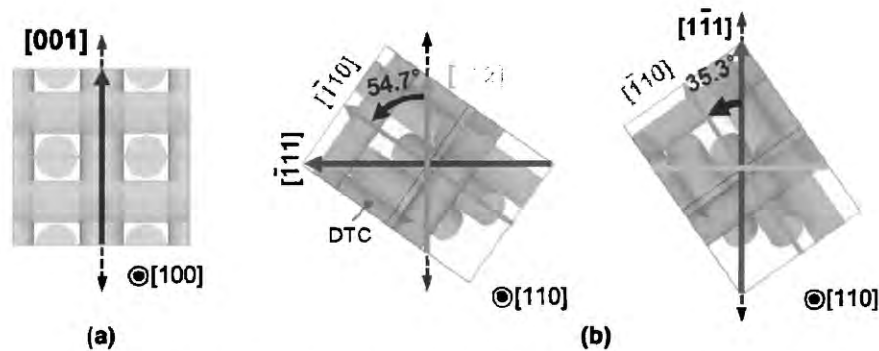
Figure 4. Schematic illustration of (a) BP II$_{(100)}$ and (b) BP I$_{(110)}$ unit cells with different azimuthal orientations. Dashed arrows indicate the orientational easy axis on the substrates.

Figure 5 shows the phase and orientation behavior of BP$_{5.0\%}$ in the rubbing and photoalignment cell. Similar to the BP$_{6.5\%}$ sample, BP I$_{(100)}$ and BP I$_{(110)}$ are obtained in the heating and cooling phases, respectively. Interestingly, the azimuthal orientation of BP I$_{(110)}$ is concentrated around approximately 36° for both rubbing and photoalignment cells, which is the same behavior found for the photoalignment cell in the BP$_{6.5\%}$ sample. The results show that for BP I grown from the isotropic phase, (110) orientation with the [1$\bar{1}$1] axis oriented along the easy axis is most stable. The results again highlight the impact of the preceding structure on BP alignment, since the behavior is different when the material exhibits BP II.
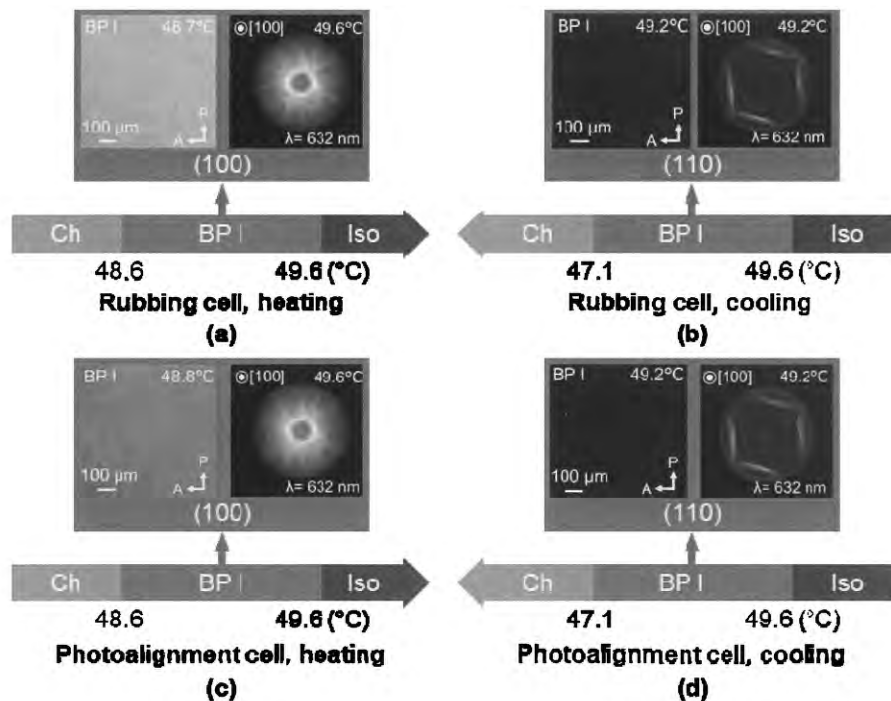

Figure 5. Phase sequence, POM image and Kossel diagrams of BP$_{5.0\%}$, which does not show BP II. (a) Heating and (b) cooling processes of the rubbing cell, and (c) heating and (d) cooling process of the photoalignment cell.

4. CONCLUSIONS

Observation of the three-dimensional crystal orientation of BPs on unidirectionally orienting surfaces revealed a strong hysteresis in alignment depending on the structure of the preceding phase. Upon BP II $\rightarrow$ I transition, a rotation in the crystal was observed such that the <100> axes of BP II coincide with the <110>, <111>, and <211> axes of BP I. Although the history of BPs goes back to the discovery of liquid crystals in 1888 when Reinitzer observed "a bright blue-violet color phenomenon" in cholesteryl benzoate [1], their alignment phenomenon is still elusive, as demonstrated by the complex behavior even on unidirectionally orienting surfaces. We believe that there is much further to investigate, such as the effect of molecular structure (both liquid crystal and alignment layer) and external fields, both experimentally and theoretically, to understand and control the alignment of these fascinating LCs.

ACKNOWLEDGMENTS

REFERENCES

[1] Seideman, T., "The liquid-crystalline blue phases", Rep. Prog. Phys. 53, 659-705 (1990).
[2] Kikuchi, H., Yokota, M., Hisakado, Y., Yang, H., & Kajiyama, T., "Polymer-stabilized liquid crystal blue phases", Nat. Mater. 1, 64-68 (2002).
[3] Yoshida, H., Tanaka, Y., Kawamoto, K., Kubo, H., Tsuda, T., Fuji, A., Kuwabata, S., Masanori, H. K. a., "Nanoparticle-stabilized cholesteric blue phases", Appl. Phys. Express 2, 121501 (2009).
[4] Jo, S., Jeon, S., Kim, B., Bae, J., Araoka, F., Choi, S-W., "Polymer stabilization of liquid-crystal blue phase II toward photonic crystals", ACS Appl. Mater. Interfaces 9, 8941-8947 (2017).
[5] Kitzerow, H. S., "The effect of electric fields on blue phases", Mol. Cryst. Liq. Cryst. 202, 51-83 (1990).
[6] Kleiman, R. N., Bishop, D. J., Pindak, R., & Taborek, P., "Shear modulus and specific heat of the liquid-crystal blue phases", Phys. Rev. Lett. 53, 2137 (1984).
[7] Hisakado, Y., Kikuchi, H., Nagamura, T., & Kajiyama, T., "Large electro-optic Kerr effect in polymer-stabilized liquid-crystalline blue phases", Adv. Mater. 17, 96-98 (2005).
[8] Heppke, G., Kitzerow, H. -S., & Krumry, M., "Electric field induced variation of the refractive index in cholesteric blue phases", Mol. Cryst. Liq. Cryst. Lett. 2, 59-65 (1985).
[9] Oton, E., Netter, E., Nakano, T., D-Katayama, Y., & Inoue, F., "Monodomain blue phase liquid crystal layers for phase modulation", Sci. Rep. 7, 44575 (2017).
[10] Etchegoin, P., "Blue phases of cholesteric liquid crystals as thermotropic photonic crystals", Phys. Rev. E 62, 1435 (2000).
[11] Lee, M., Chang, C., & Lee, W., "Label-free protein sensing by employing blue phase liquid crystal", Biomed. Opt. Express 8, 1712-1720 (2017).
[12] Kawata, Y., Yoshida, H., Tanaka, S., Anucha, K., Ozaki, M., & Kikuchi, H., "Anisotropy of the electro-optic Kerr effect in polymer-stabilized blue phases", Phys. Rev. E 91, 022503 (2015).
[13] Chen, P., Chen, M., Ni, S., Chen, H., & Lin, Y., "Influence of alignment layers on crystal growth of polymer-stabilized blue phase liquid crystals", Opt. Mater. Express 6, 1003-1010 (2016).
[14] Chen, Y., & Wu, S., "Electric field-induced monodomain blue phase liquid crystals", Appl. Phys. Lett. 102, 171110 (2013).
[15] Takahashi, M., Ohkawa, T., Yoshida, H., Fukuda, J., Kikuchi, H., & Ozaki, M., "Orientation of liquid crystalline blue phases on unidirectionally orienting surfaces", J. Phys. D: Appl. Phys. 51, 104003 (2018).

[16] Chen, H., Lin, Y., Wu, C., Chen, . M., & Hsu, H., "Hysteresis-free polymer-stabilized blue phase liquid crystals using thermal recycles", Opt. Mater. Express 2, 1149-1155 (2012).

[17] Yoshida, H., Anucha, K., Ogawa, Y., Kawata, Y., Fukuda, J., Kikuchi, H., & Ozaki, M., "Bragg reflection band width and optical rotatory dispersion of cubic blue phase liquid crystals", Phys. Rev. E 94, 042703 (2016).

[18] Li, X., Martínez-González, J. A., Hernández-Ortiz, J. P., Ramírez-Hernández, A., Zhou, Y., Sadati, M., Zhang, R., Nealey, P. F., & de Pabo, J. J., "Mesoscale martensitic transformation in single crystals of topological defects", Proc. Nat. Acad. Sci. 114, 10011-10016 (2017).

[19] Tanaka, S., Yoshida, H., Kawata, Y., Kuwahara, R., Nishi, R., & Ozaki, M., "Double-twist cylinders in liquid crystalline cholesteric blue phases observed by transmission electron microscopy", Sci. Rep. 5, 16180 (2015).